Redox Chemistry of Water-Soluble Iron, Manganese, and Chromium Metalloporphyrins and Acid–Base Behavior of Their Lyate Axial Ligands in Aqueous Solution: Influence of Electronic Effects

Seungwon Jeon and Thomas C. Bruice*

Department of Chemistry, University of California at Santa Barbara, Santa Barbara, California 93106

Received January 29, 1992

Electrochemical oxidation and reduction of water-soluble and non-μ-oxo dimer-forming [5,10,15,20-tetrakis(2,6-dichloro-3-sulfonatophenyl)porphyrinato]iron(III) {(**2**)$Fe^{III}(X)_2$}, -manganese(III) {(**2**)$Mn^{III}(X)_2$}, and -chromium(III) {(**2**)$Cr^{III}(X)_2$} (where X = H_2O or HO^-) hydrates have been investigated in aqueous solutions as a function of pH. The midpoint potentials for the stepwise 1e$^-$ oxidations and reductions of (**2**)$Fe^{III}(X)_2$ shift to more positive values compared to those of [5,10,15,20-tetrakis(2,6-dimethyl-3-sulfonatophenyl)porphyrinato]iron(III) {(**1**)$Fe^{III}(X)_2$}, and the pK_a values (4.1 and 7.8) for the acid dissociation of the H_2O molecules axially ligated to (**2**)$Fe^{III}(H_2O)_2$ have lower values than those (6.55 and 10.55) for (**1**)$Fe^{III}(H_2O)_2$ due to the inductive effects of the 2,6-dichloro substituents of (**2**)$Fe^{III}(H_2O)_2$ compared to the 2,6-dimethyl substituents of (**1**)$Fe^{III}(H_2O)_2$. Values of formal potentials for the interconversion of the iron(III) and iron(IV) porphyrin hydrates are $e^- + $ (**2**)$Fe^{IV}(H_2O)_2 \rightleftarrows$ (**2**)$Fe^{III}(H_2O)_2$, 1.20 V; $e^- +$ (**2**)$Fe^{IV}(H_2O)(OH) \rightleftarrows$ (**2**)$Fe^{III}(H_2O)(OH)$, 1.10 V; $e^- +$ (**2**)$Fe^{IV}(OH)_2 \rightleftarrows$ (**2**)$Fe^{III}(OH)_2$, 1.06 V. Spectroelectrochemical investigations of the controlled-potential 1e$^-$ oxidation of (**2**)$Fe^{III}(X)_2$ show that the various iron(IV) species, formed at different pHs, have the same spectral characteristics as seen previously in the oxidation of (**2**)$Fe^{III}(X)_2$ by *tert*-butyl hydroperoxide in aqueous solution. The half-wave potential (1.34 V) for the 1e$^-$ oxidation of (**2**)$Fe^{IV}(X)_2$ to (**2**$^{\cdot+}$)$Fe^{IV}(X)_2$ is pH independent, due to the equality of the pK_a values of water ligated to the iron(IV) porphyrin and iron(IV) porphyrin π-cation radical. The pK_{a1} (4.4) of (**2**)$Mn^{III}(H_2O)_2$ is smaller than the pK_{a1} (5.8) of (**1**)$Mn^{III}(H_2O)_2$, and the formal potentials for 1e$^-$ oxidation of (**2**)$Mn^{III}(X)_2$ are 1.20 V for (**2**)$Mn^{III}(H_2O)_2$ and 1.05 V for (**2**)$Mn^{III}(H_2O)(OH)$. Likewise, the pK_a values (8.0 and 10.4) of (**2**)$Cr^{III}(H_2O)_2$ are smaller than those (9.4 and 12.4) for (**1**)$Cr^{III}(H_2O)_2$, and the formal potentials for 1e$^-$ oxidation of (**2**)$Cr^{III}(X)_2$ are 0.71 V for (**2**)$Cr^{III}(H_2O)_2$, 0.63 V for (**2**)$Cr^{III}(H_2O)(OH)$, and 0.56 V for (**2**)$Cr^{III}(OH)_2$. The differences in pK_a values and formal potentials between (**2**)$M^{III}(X)_2$ (M = Fe, Mn, or Cr) and (**1**)$M^{III}(X)_2$ are discussed in view of the inductive effects rather than the field effects of phenyl substituents of metallo-5,10,15,20-tetrakis(phenyl)porphyrins on the metalloporphyrin moiety.

Introduction

By determining[1] the pH dependence of electrode potentials of iron, manganese, and chromium complexes of the water-soluble 5,10,15,20-tetrakis(2,6-dimethyl-3-sulfonatophenyl)porphyrin {(**1**)H_2}, we have defined the formal potentials of formation of the various oxidation states as well as the pK_a values of water molecules which are axial ligands. Redox reactions involving iron and manganese are of significance in the chemistries of peroxidases,[2] catalases,[3] cytochrome P-450s,[4] superoxide dismutases,[5] and photosynthesis.[6]

We report here an investigation of the pH dependence of the oxidation and reduction potentials and associated pK_a values for the water-soluble and non-μ-oxo dimer-forming [5,10,15,20-tetrakis(2,6-dichloro-3-sulfonatophenyl)porphyrinato]iron(III) {(**2**)$Fe^{III}(X)_2$}, -manganese(III) {(**2**)$Mn^{III}(X)_2$}, and -chromium(III) {(**2**)$Cr^{III}(X)_2$} (where X = H_2O or HO^-) hydrates in aqueous solutions. The oxidation states investigated extend from 2e$^-$ reduction to 2e$^-$ oxidation of (**2**)$M^{III}(X)_2$ (M = Fe, Mn, or Cr) when the axial ligands $(X)_2$ are $(H_2O)_2$, $(H_2O)(OH)$, and in some cases $(OH)_2$. In previous studies[1a-c] there has been collected like electrochemical measurements with [5,10,15,20-tetrakis(2,6-dimethyl-3-sulfonatophenyl)porphyrinato]iron(III) {(**1**)$Fe^{III}(X)_2$}, -manganese(III) {(**1**)$Mn^{III}(X)_2$}, and -chromium(III) {(**1**)$Cr^{III}(X)_2$} (where X = H_2O or HO^-) hydrates in aqueous solution. Substitution of the eight *o*-chloro groups of (**2**)$M^{III}(X)_2$ with eight *o*-methyl substituents provides (**1**)$M^{III}(X)_2$ (see Chart I). In previous investigations[9a,13a] the pK_a values of H_2O ligated to iron(III) porphyrins were spectrophotometrically determined as 6.6 with (**1**)$Fe^{III}(H_2O)_2$ and 7.6 with (**2**)$Fe^{III}(H_2O)_2$, respectively. The apparently higher pK_a for (**2**)$Fe^{III}(H_2O)_2$ was explained as the influence of a field effect on the ligated water by the closely adjacent *o*-chloro substituents. In the present study we find an electrochemically evident (but spectrophotometrically invisible) pK_a of 4.1 for (**2**)$Fe^{III}(H_2O)_2$,

(1) (a) Kaaret, T. W.; Zhang, G.-H.; Bruice, T. C. *J. Am. Chem. Soc.* **1991**, *113*, 4652. (b) Jeon, S.; Bruice, T. C. *Inorg. Chem.* **1991**, *30*, 4311. (c) Arasasingham, R. D.; Jeon, S.; Bruice, T. C. *J. Am. Chem. Soc.* **1992**, *114*, 2536.

(2) (a) Dunford, H. B.; Stillman, J. S. *Coord. Chem. Rev.* **1976**, *19*, 187. (b) Hewson, W. D.; Hager, L. D. *Porphyrins* **1979**, *7*, 295. (c) Dunford, H. B. *Adv. Inorg. Biochem.* **1982**, *4*, 41. (d) Gold, M. H.; Wariishi, H.; Valli, K. *ACS Symp. Ser.* **1989**, *389*, 127. (e) Guengerich, F. P. *Crit. Rev. Biochem. Mol. Biol.* **1990**, *25*, 97.

(3) (a) Hrycay, E. G.; O'Brien, P. J. *Arch. Biochem. Biophys.* **1971**, *147*, 4. (b) Kadlubar, K. C.; Morton, K. C.; Ziegler, D. M. *Biochem. Biophys. Res. Commun.* **1973**, *54*, 1255. (c) Hrycay, E. G.; O'Brien, P. J. *Arch. Biochem. Biophys.* **1974**, *160*, 230. (d) Nordblom, G. D.; White, R. E.; Coon, M. J. *Arch. Biochem. Biophys.* **1976**, *175*, 524. (e) Blake, R. C.; Coon, M. J. *J. Biol. Chem.* **1981**, *256*, 12127. (f) Kono, Y.; Fridovich, I. *J. Biol. Chem.* **1983**, *258*, 6015. (g) McCarthy, M. B.; Whiter, R. E. *J. Biol. Chem.* **1983**, *258*, 9135. (h) Beyer, W. F.; Fridovich, I. *Biochemistry* **1985**, *24*, 6460. (i) Beyer, W. F.; Fridovich, I. In *Oxygen Radicals in Biology and Medicine*; Simic, M. G.; Taylor, K. A., Ward, J. F., von Sanntag, C., Eds.; Plenum: New York, 1988; p 651. (j) Fronko, R. M.; Penner-Hahn, J. E.; Bender, C. J. *J. Am. Chem. Soc.* **1988**, *110*, 7554.

(4) (a) Kaufman, S.; Fisher, D. B. In *Molecular Mechanisms of Oxygen Activation*; Hayaishi, O., Ed.; Academic: New York, 1974; p 286. (b) Siegal, B. *Bioorg. Chem.* **1979**, *8*, 219.

(5) Michaelson, A. M.; McCord, J. M.; Fridovich, I., Eds. *Superoxide and Superoxide Dismutases*; Academic Press: New York, 1977.

(6) (a) Kok, B.; Forbush, B.; McGloin, M. *Photochem. Photobiol.* **1970**, *11*, 457. (b) Livorness, J.; Smith, T. D. *Struct. Bonding* **1982**, *48*, 1. (c) Renger, G.; Govindjee. *Photosynth. Res.* **1985**, *6*, 33. (d) Dismukes, G. C. *Photochem. Photobiol.* **1986**, *43*, 99. (e) Renger, G. *Angew. Chem., Int. Ed. Engl.* **1987**, *26*, 643.

(7) Lindsey, J. S.; Wagner, R. W. *J. Org. Chem.* **1989**, *54*, 828.

0020-1669/92/1331-4843$03.00/0

Chart I

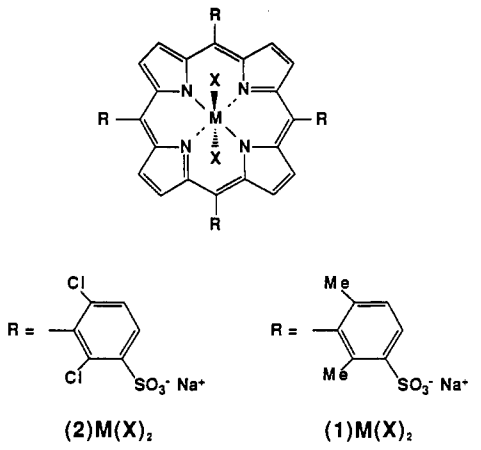

(2)M(X)$_2$ (1)M(X)$_2$

negating the requirements for other than inductive effects of substituents. Comparison of the acid–base and electrochemical properties of (**2**)M^{III}(X)$_2$ and (**1**)M^{III}(X)$_2$ allows a quantitative assessment of the influence of the electronic effects of phenyl substituents of metallo-5,10,15,20-tetrakis(phenyl)porphyrins on the metalloporphyrin moiety. This is the first investigation which involves such comparisons in aqueous solution without the intervention of stacking and μ-oxo dimer formation above pH 7.0. A knowledge of the acid–base properties and electrochemical potentials of(**1**)M^n(X)$_2$ and (**2**)M^n(X)$_2$ species will be invaluable to future studies which involve the acidity dependence of reactions of iron, manganese, and chromium porphyrins in aqueous solution.

Experimental Section

Almost all the electrochemical measurements, instrumentation, and materials have been reported previously.[1]

Porphyrin Synthesis. 5,10,15,20-Tetrakis(2,6-dichlorophenyl)porphyrin was synthesized by condensing 2,6-dichlorobenzaldehyde and pyrrole according to the method of Lindsey et al.[7] and converted to 5,10,15,20-tetrakis(2,6-dichloro-3-sulfonatophenyl)porphyrin {(**2**)H$_2$} by the procedure of Dolphin et al.[8] [5,10,15,20-Tetrakis(2,6-dichloro-3-sulfonatophenyl)porphyrinato]iron(III) hydrate {(**2**)Fe^{III}(H$_2$O)$_2$} and -manganese(III) hydrate {(**2**)Mn^{III}(H$_2$O)$_2$} were from the previous studies.[9] The insertion of chromium was accomplished by the method described by Garrison et al.[10] [5,10,15,20-Tetrakis(2,6-dichloro-3-sulfonatophenyl)porphyrinato]chromium(III) hydrate {(**2**)Cr^{III}(H$_2$O)$_2$} was prepared by refluxing the free base with a 40-fold excess of chromium(II) chloride in DMF for 2 h. The water-soluble (**2**)Cr^{III}(H$_2$O)$_2$ was purified by ion exchange, ultrafiltration, and size-exclusion chromatography.

Electrochemical Measurements. All aqueous solutions used for electrochemistry were prepared from distilled-deionized water. Preparations of all solutions were carried out under an argon atmosphere scrubbed free of O_2. Dilute solutions of carbonate-free HNO_3 and NaOH were used for the adjustment of pH. The measured pH values were within ±0.05 pH units. All reported potentials are with respect to the saturated calomel electrode (SCE). The ionic strength was maintained at 0.2 with $NaNO_3$ or $NaClO_4$.

Instrumentation. The cyclic voltammetric measurements were accomplished with a three-electrode potentiostat (Bioanalytical Systems, Model CV-27) and a Houston Instruments Model 100 Omnigraphic recorder. A glassy-carbon electrode (surface area 0.062 cm^2) was employed as the working electrode for the determination of the pH dependence of electrode potential in aqueous solutions. All working electrode surfaces were highly polished with Al_2O_3 paste prior to each experiment. A Pt-mesh working electrode was used in spectroelectrochemical experiments. Absorption spectra were recorded on a Cary 14 spectrophotometer interfaced to a Zenith computer equipped with OLIS (On-Line Instrument System Inc.) data acquisition and processing software.

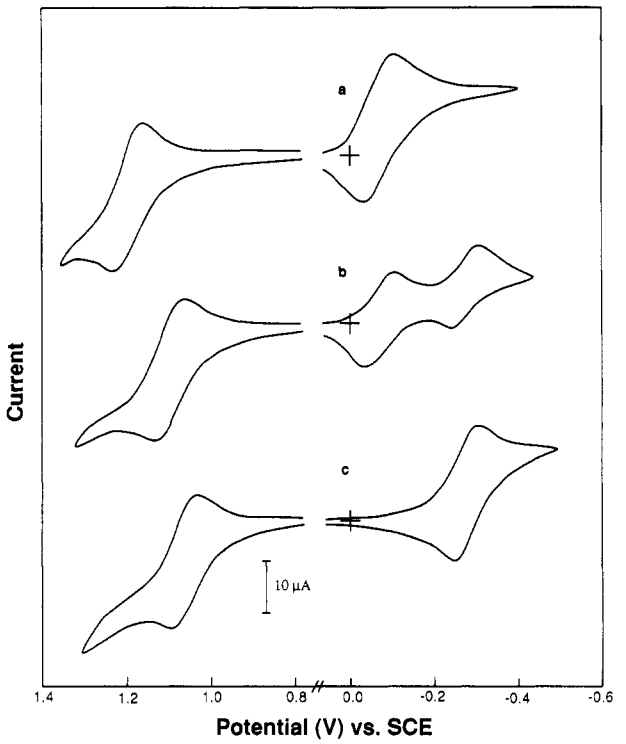

Figure 1. Cyclic voltammograms for the oxidation and reduction of 3.1 mM (**2**)Fe^{III}(X)$_2$ in water (0.2 N $NaNO_3$) at various pH values at a scan rate 0.1 V s^{-1}: (a) pH 2.1; (b) pH 6.5; (c) pH 9.5.

Results

The pH dependence of the potentials for oxidation and reduction of (2)Fe^{III}(X)$_2$ in aqueous solutions (μ = 0.2 with $NaNO_3$) was examined between pH 1.4 and 10.0 under an argon atmosphere. Cyclic voltammograms, at different pH values, obtained by use of a polished glassy-carbon electrode are shown in Figure 1. Scanning at 0.1 V s^{-1}, a plot of the half-wave potential {E_m = ($E_{p,a}$ + $E_{p,c}$)/2} vs pH for the oxidation of (**2**)Fe^{III}(X)$_2$ is shown in Figure 2. The E_m for the first oxidation of (**2**)Fe^{III}(X)$_2$ is constant at constant pH within the scan rate used (scan rate, 20–200 mV/s), but the peak separation (ΔE) between $E_{p,a}$ and $E_{p,a}$ slightly increases with scan rate as 62 mV with 20 mV/s and 75 mV with 200 mV/s. This well-defined first oxidation wave of (**2**)Fe^{III}(X)$_2$ is quasi-reversible. The dependence of the anodic peak current ($i_{p,a}$) as a function of the square root of the scan rate (v) is linear, as expected from a diffusion-controlled process. The half-wave potential of the first oxidation of (**2**)Fe^{III}(X)$_2$ shifts from 1.20 V below pH 2.3 to 1.06 V above pH 7.8. Three plateau regions (Figure 2a) are observed, one below pH 2.3, a second plateau between pH 4.1 and 7.1 with a potential of 1.10 V, and a third one above pH 7.8. Between pH 2.3 and 4.1 and pH 7.1 and 7.8 the half-wave potentials decrease with a slope of about 60 mV/pH unit. The half-wave potential of the second oxidation of (**2**)Fe^{III}(X)$_2$ is pH independent with a value of 1.34 V (Figure 2b). Cyclic voltammetry at pH >10 yielded unsatisfactory voltammetric responses due to the intervention of the oxidation of hydroxide ion.

The characterization of the anodic product of (**2**)Fe^{III}(X)$_2$ was studied by thin-layer spectroelectrochemistry using a platinum-

(8) Dolphin, D.; Nakano, T.; Maione, T. E.; Kirk, T. K.; Farrell, R. In *Synthetic Model Ligninases*; Odier, E., Ed.; Lignin Enzymic and Microbial Degradation; INRA Publications: Paris, 1987; p 157.
(9) (a) Panicucci, R.; Bruice, T. C. *J. Am. Chem. Soc.* **1990**, *112*, 6063. (b) Murata, K.; Panicucci, R.; Gopinath, E.; Bruice, T. C. *J. Am. Chem. Soc.* **1990**, *112*, 6072. (c) Arasasingham, R. D.; Bruice, T. C. *J. Am. Chem. Soc.* **1991**, *113*, 6095.
(10) Garrison, J. M.; Lee, R. W.; Bruice, T. C. *Inorg. Chem.* **1990**, *29*, 2019.
(11) (a) Harriman, A. *J. Chem Soc., Dalton Trans.* **1984**, 141. (b) Bettelheim, A.; Ozer, D.; Weinraub, D. *J. Chem. Soc., Dalton Trans.* **1986**, 2297.
(12) Clark, W. M. In *Oxidation-Reduction Potentials of Organic Systems*; Krieger, R. E., Ed.; Huntington, NY, 1972; Chapter 4.
(13) (a) Zipplies, M. F.; Lee, W. A.; Bruice, T. C. *J. Am. Chem. Soc.* **1986**, *108*, 4433. (b) Gopinath, E.; Bruice, T. C. *J. Am. Chem. Soc.* **1991**, *113*, 4657.

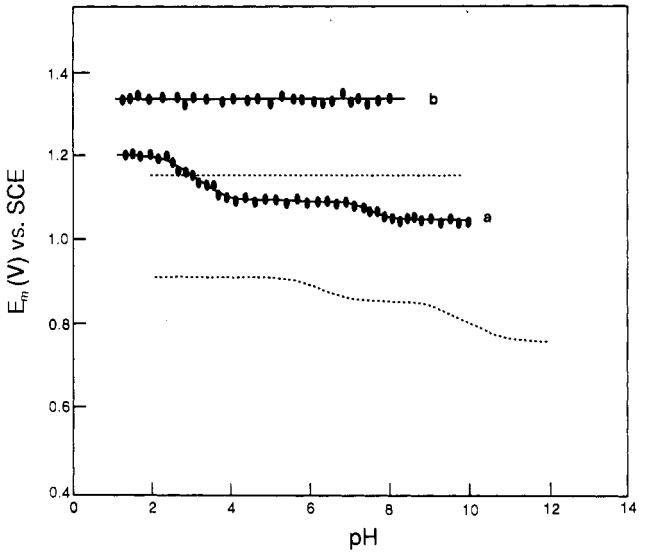

Figure 2. Nernst–Clark plots of the (2)$Fe^{III}(X)_2$ half-wave potential (E_m) vs pH determined at 0.1 V s^{-1} with a glassy-carbon electrode: (a) $1e^-$ oxidation of (2)$Fe^{III}(X)_2$; (b) $1e^-$ oxidation of (2)$Fe^{IV}(X)_2$. Solid lines represent theoretical fits to the experimental points. Dashed lines represent plots of E_m vs pH for (1)$Fe^{III}(X)_2$ (from ref 1a).

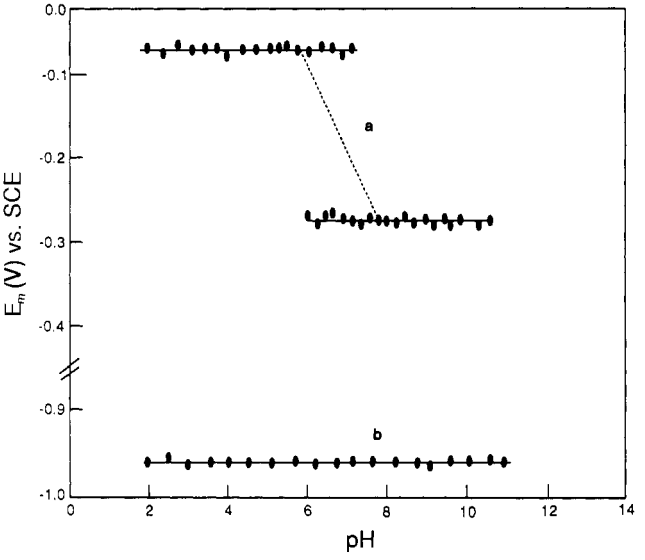

Figure 3. Nernst–Clark plots of the (2)$Fe^{III}(X)_2$ half-wave potential (E_m) vs pH determined at 0.1 V s^{-1} with a glassy-carbon electrode: (a) $1e^-$ reduction of (2)$Fe^{III}(X)_2$; (b) $1e^-$ reduction of (2)$Fe^{II}(X)$. Solid lines represent theoretical fits to the experimental points.

minigrid electrode. Spectroelectrochemical controlled-potential $1e^-$ oxidation between pH 5 and 10, conducted 250 mV more positive than E_m for the oxidation of (2)$Fe^{III}(X)_2$, shows the same spectral changes which accompany oxidation of (2)$Fe^{III}(X)_2$ by *tert*-butyl hydroperoxide.[9b] The Soret band at 423 nm diminishes as the absorbance at 430 nm increases during incremental $1e^-$ oxidation of (2)$Fe^{III}(X)_2$ above pH 7.5. Below pH 7.5, $1e^-$ oxidation results in decreases in absorbance at 403 and 423 nm, and by pH 5, much iron porphyrin is lost.

A plot of half-wave potential vs pH for the reduction of (2)-$Fe^{III}(X)_2$ is shown in Figure 3. The E_m for the first reduction shifts from –0.07 V below pH 6 to –0.27 V above pH 7. The measured current below pH 6 corresponds (within experimental error) to a $1e^-$ reduction of (2)$Fe^{III}(X)_2$, as established by a comparison to the current measured for the $1e^-$ oxidation of (2)-$Fe^{III}(X)_2$ at the same pH (see Figure 1). Below pH 6 the half-wave potential is constant at –0.07 V, and above pH 7 it is constant at –0.27 V (Figure 3a). However, between pH 6 and 7 two reduction waves are observed, and the sum of the two currents

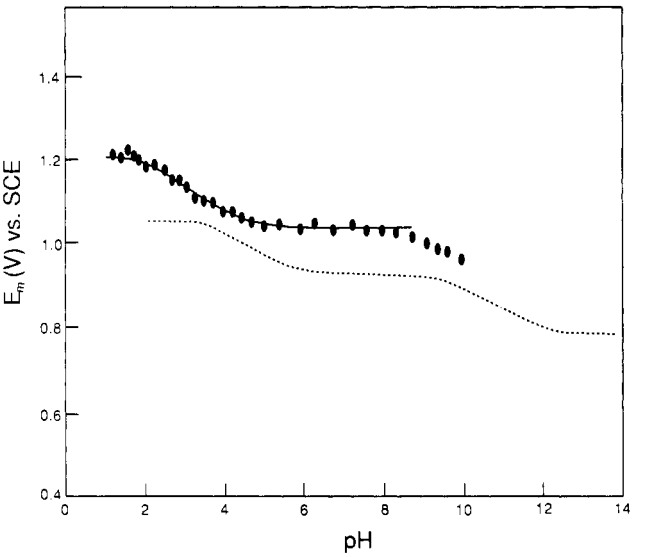

Figure 4. Nernst–Clark plots of the $1e^-$ oxidation of (2)$Mn^{III}(X)_2$ half-wave potential (E_m) vs pH determined at 0.1 V s^{-1} with a glassy-carbon electrode. The solid line represents the theoretical fit of the Nernst–Clark equation to the experimental points. For comparison the dashed lines represent plots of E_m vs pH for (1)$Mn^{III}(X)_2$ (from ref 1a).

for the two waves is equal to a $1e^-$ reduction. As the pH is increased from 6 to 7, the current associated with the reduction at –0.07 V decreases in magnitude, while that associated with the reduction at –0.27 V increases. By thin-layer spectroelectrochemical experiments, the disappearance of the Soret band during $1e^-$ reduction of (2)$Fe^{III}(X)_2$ is accompanied by the appearance of a peak at 439 nm between pH 2 and 10. The second reduction of (2)$Fe^{III}(X)_2$ is pH independent (Figure 3b) with an E_m of –0.95 V.

The pK_a value of (2)$Fe^{III}(X)_2$ in aqueous solutions (μ = 0.2 with $NaNO_3$) was measured by spectrophotometric titration at 403 and 423 nm between pH 2 and 12. The least-squares pK_a of 7.6 ± 0.1 was determined by the fitting of the change of absorbance with pH to a theoretical curve for acid dissociation of a monoprotic acid.

The pH dependence of the oxidation potential of (2)$Mn^{III}(X)_2$ in aqueous solutions (μ = 0.2 with $NaNO_3$) was examined between pH 1.2 and 10.0 under an argon atmosphere. Scanning with a glassy-carbon electrode at 0.1 V s^{-1} yields the plot of E_m vs pH shown in Figure 4. The half-wave potential of the oxidation of (2)$Mn^{III}(X)_2$ shifts from 1.20 V below pH 1.8 to 0.97 V at pH 10.0. Two plateau regions are observed, one with a potential at 1.20 V below pH 1.8 and a second plateau between pH 4.4 and 8.0 with a potential of 1.05 V. Between pH 1.8 and 4.4 the E_m decreases with a slope of about 60 mV/pH unit.

Thin-layer coulometric experiments show that the first oxidation of (2)$Mn^{III}(X)_2$ between pH 1.5 and 10.0 is a $1e^-$ process (n = 1.02 ± 0.05). Spectroelectrochemical observations during $1e^-$ oxidation of (2)$Mn^{III}(X)_2$ parallel spectral observations recorded for the oxidation of (2)$Mn^{III}(X)_2$ by $(Ph_2)_2$(MeOCO)-COOH.[9c] The disappearance of the Soret band (470 nm) by $1e^-$ oxidation of (2)$Mn^{III}(X)_2$ at pH 8.9 is accompanied by the formation of (2)$Mn^{IV}(X)_2$ absorbing at 423 nm. The electrochemically generated manganese(IV) moiety has an absorption spectrum nearly identical with that generated by the reaction of $(Ph_2)_2$(MeOCO)COOH with (2)$Mn^{III}(X)_2$ at pH 8.9. The electronic spectra of (2)$Mn^{III}(X)_2$ and (2)$Mn^{IV}(X)_2$ are similar to that cited in the literature for manganese(III) and manganese-(IV) cationic water-soluble tetraarylporphyrins.[11]

The pH dependence of the oxidation and reduction potentials of (2)$Cr^{III}(X)_2$ in aqueous solutions (μ = 0.2 with $NaClO_4$) was examined between pH 2.0 and 11.5 under an argon atmosphere. The half-wave potential of the first oxidation of (2)$Cr^{III}(X)_2$ at

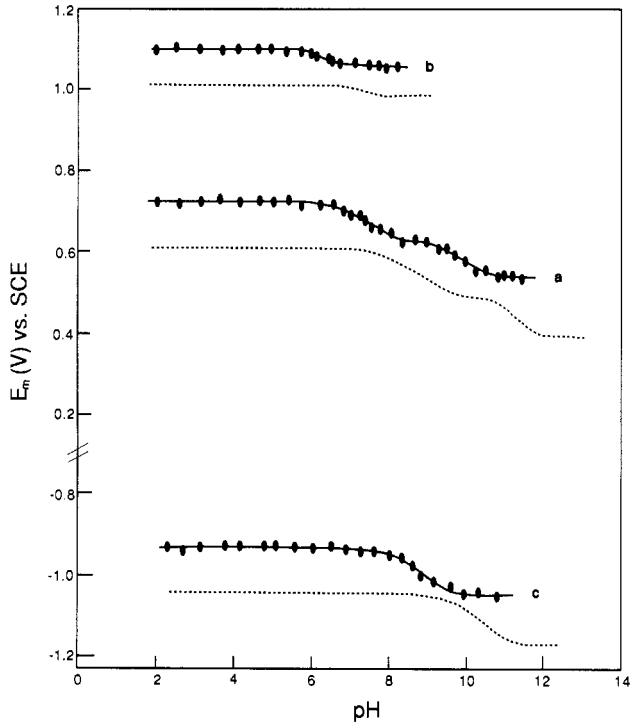

Figure 5. Nernst–Clark plots of the (2)$Cr^{III}(X)_2$ half-wave potential (E_m) vs pH determined at 0.1 V s^{-1} with a glassy-carbon electrode: (a) $1e^-$ oxidation of (2)$Cr^{III}(X)_2$; (b) $1e^-$ oxidation of (2)$Cr^{IV}(X)_2$; (c) $1e^-$ reduction of (2)$Cr^{III}(X)_2$. Solid lines represent theoretical fits to the experimental points. For comparison, dashed lines represent comparable Nernst–Clark plots of E_m vs pH for the $1e^-$ oxidation of (1)$Cr^{III}(X)_2$, $1e^-$ oxidation of (1)$Cr^{IV}(X)_2$, and $1e^-$ reduction of (1)$Cr^{III}(X)_2$ (from ref 1b).

a scan rate of 0.1 V s^{-1} shifts from 0.71 V below pH 6.5 to 0.56 V above pH 10.4. A plot of E_m vs pH is shown in Figure 5. Three plateau regions are observed in the first oxidation of (2)$Cr^{III}(X)_2$ (Figure 5a), one below pH 6.5, a small second plateau between pH 8.0 and 8.9 with a potential of 0.63 V, and a third one above pH 10.4. Between pH 6.5 and 8.0 and pH 8.9 and 10.4 the half-wave potential decreases with a slope of about 60 mV/pH unit. The half-wave potential of the second oxidation of (2)-$Cr^{III}(X)_2$ is slightly pH dependent between pH 6.0 and 6.5 (Figure 5b).

Thin-layer coulometric experiments show that the first oxidation of (2)$Cr^{III}(X)_2$ is a $1e^-$ process (n = 1.01 ± 0.04). The disappearance of the Soret band (447 nm below pH 7, 439 nm above pH 9) by $1e^-$ oxidation of (2)$Cr^{III}(X)_2$ is accompanied by the formation of (2)$Cr^{IV}(X)_2$ absorbing at 423 nm.

The half-wave potential of the first reduction of (2)$Cr^{III}(X)_2$ shifts from –0.96 V below pH 8.0 to –1.04 V above pH 9.3 (Figure 5c). The half-wave potential decreases with a slope of 65 mV/pH between pH 8.0 and 9.3. The first reduction current of (2)-$Cr^{III}(X)_2$ is comparable to the current measured for the first oxidation of (2)$Cr^{III}(X)_2$ which establishes the first reduction to involve a $1e^-$ transfer reaction.

The pK_a value of (2)$Cr^{III}(X)_2$ in aqueous solutions (μ = 0.2 with $NaClO_4$) was determined to be 8.1 ± 0.1 by spectrophotometric titration at 447 and 439 nm between pH 3 and 12. From the spectrophotometric titration data the following characteristics are assigned to the various chromium(III) porphyrin species: (2)-$Cr^{III}(H_2O)_2$ (pH 5.45) λ_{max} = 447 nm, $\epsilon = 7.7 \times 10^4$ M^{-1} cm^{-1}; (2)$Cr^{III}(H_2O)(OH)$ (pH 9.53) λ_{max} = 439 nm, $\epsilon = 8.4 \times 10^4$ M^{-1} cm^{-1}.

Discussion

The pH dependence of the oxidation and reduction potentials of the hydrates of [5,10,15,20-tetrakis(2,6-dichloro-3-sulfonatophenyl)porphyrinato]iron(III) {(2)$Fe^{III}(X)_2$}, -manganese(III) {(2)-$Mn^{III}(X)_2$}, and -chromium(III) {(2)$Cr^{III}(X)_2$} (where X = H_2O or HO^-) has been investigated in water as a function of pH at an ionic strength of 0.2. This class of metal(III) porphyrins does not form μ-oxo dimers due to the steric effects of the *o*-chloro substituents. Associated pK_a values and apparent formal potentials of various oxidation states of (2)$Fe(X)_2$, (2)$Mn(X)_2$, and (2)$Cr(X)_2$ have been determined from electrochemical data and may now be compared with those of various oxidation states of the hydrates of [5,10,15,20-tetrakis(2,6-dimethyl-3-sulfonatophenyl)porphyrinato]iron(III) {(1)$Fe^{III}(X)_2$}, -manganese(III) {(1)-$Mn^{III}(X)_2$}, and -chromium(III) {(1)$Cr^{III}(X)_2$} from previous studies.[1] This is the first such study to be carried out in aqueous solution.

Redox Chemistry of (2)$Fe^{III}(X)_2$. The dependence of half-wave potential upon pH for the oxidation of (2)$Fe^{III}(X)_2$ is shown in Figure 2. The lines generated to fit the experimental points were obtained by computer fitting of the appropriate Nernst–Clark equations (Scheme I) which were derived by use of the equilibria in Scheme II.[12] In order to compare the pH dependence for the potentials of (2)$Fe^{III}(X)_2$ and (1)$Fe^{III}(X)_2$ the pH dependence of E_m for the latter are included as dashed lines in Figure 2. Cyclic voltammetric and spectroelectrochemical results indicate that the $1e^-$ oxidation of (2)$Fe^{III}(X)_2$ is metal-centered and gives (2)$Fe^{IV}(X)_2$. The pH dependence of the $1e^-$ oxidation potentials establishes the correctness of the structures (2)Fe^{III}-$(H_2O)_2$, (2)$Fe^{III}(OH)(H_2O)$, and (2)$Fe^{III}(OH)_2$ and the pH dependence of their formation (Scheme II). The pH independence of the half-wave potential (1.34 V) for $1e^-$ oxidation of (2)Fe^{IV}-$(X)_2$ to ($2^{\bullet+}$)$Fe^{IV}(X)_2$ indicates that the pK_a values for water axial ligated to iron(IV) porphyrin and iron(IV) porphyrin

Scheme I

(a) for the one-electron oxidation of (2)$Fe^{III}(X)_2$

$$E_m = E^{\circ\prime} + \frac{RT}{F} \ln \left[\frac{a_{H^+}^2 + K_{a1}^{III} a_{H^+} + K_{a1}^{III} K_{a2}^{III}}{a_{H^+}^2 + K_{a1}^{IV} a_{H^+} + K_{a1}^{IV} K_{a2}^{IV}} \right]$$

(b) for the one-electron oxidation of (2)$Fe^{IV}(X)_2$

$$E_m = E^{\circ\prime} + \frac{RT}{F} \ln \left[\frac{a_{H^+}^2 + K_{a1}^{IV} a_{H^+} + K_{a1}^{IV} K_{a2}^{IV}}{a_{H^+}^2 + K_{a1}^{V} a_{H^+} + K_{a1}^{V} K_{a2}^{V}} \right]$$

Scheme II

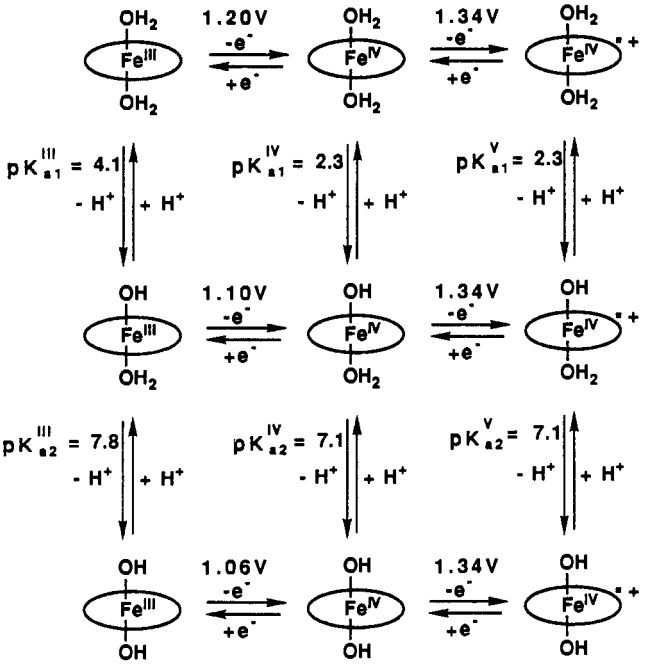

π-cation radical species must be nearly the same. The pH independence of the electrode potentials in the oxidations of (**2**)-$Fe^{IV}(X)_2$ to $(\mathbf{2}^{\bullet+})Fe^{IV}(X)_2$ is explained on the basis that the electron added to or removed from the porphyrin ring in the course of these reactions is delocalized over the porphyrin 24-atom framework such that the electron density of the Fe^{IV} water ligation center is not much altered. This electrochemical observation confirms that a $2e^-$ oxidation of an oxo-ligated iron(III) porphyrin provides an iron(IV) porphyrin π-cation radical rather than an iron(V) porphyrin.[14] Formation of an iron(V) porphyrin would lower the pK_a of ligated water relative to that of the iron(IV) porphyrin due to the increased electropositivity of the iron and the driving force to reach electroneutrality in the iron moiety. Like conclusions were reached in the oxidations of (**1**)$Fe^{IV}(X)_2$.[1a] The acid dissociation constants for (**2**)$Fe^{III}(H_2O)_2$, (**2**)$Fe^{IV}(H_2O)_2$, and $(\mathbf{2}^{\bullet+})Fe^{IV}(H_2O)_2$ obtained from the best fit of the appropriate Nernst–Clark equations to the experimental points of Figure 2 are provided in Scheme II.

The pK_{a1} of (**2**)$Fe^{III}(H_2O)_2$ was electrochemically measured to be 4.1 ± 0.2. This acid dissociation constant cannot be observed by spectrophotometric acid–base titration due to the close similarity of the spectra of (**2**)$Fe^{III}(H_2O)_2$ and (**2**)$Fe^{III}(H_2O)$-(OH). Interestingly, the pK_{a1} of (**1**)$Fe^{III}(H_2O)_2$ can be determined by spectrophotometric titration.[13] The electrochemically measured pK_{a2} of 7.8 ± 0.2 for (**2**)$Fe^{III}(H_2O)(OH)$ compares favorably to that (7.6 ± 0.1) determined by spectrophotometric titration at an ionic strength of 0.2. The observation of spectral changes at pK_{a1} with (**1**)$Fe^{III}(H_2O)_2$ but not with (**2**)$Fe^{III}(H_2O)_2$ and spectral changes at pK_{a2} with (**2**)$Fe^{III}(H_2O)(OH)$ but not with (**1**)$Fe^{III}(H_2O)(OH)$ suggests that either the spin state of Fe(III) or the conformation of the porphyrin moiety in (**2**)$Fe^{III}(X)_2$ has a dependence on pH which is different compared to (**1**)$Fe^{III}(X)_2$. The half-wave potentials at the three pH-independent regions in the plot of E_m vs pH for $1e^-$ oxidation of (**2**)$Fe^{III}(X)_2$ can be thought of as apparent formal potentials ($E°'$) for the oxidation–reduction equilibria between (**2**)$Fe^{III}(X)_2$ and (**2**)$Fe^{IV}(X)_2$, as shown in Scheme II. For comparison the apparent formal potentials for $1e^-$ oxidation of (**1**)$Fe^{III}(X)_2$ are 0.91 V for (**1**)$Fe^{III/IV}(H_2O)_2$, 0.86 V for (**1**)$Fe^{III/IV}(H_2O)(OH)$, and 0.77 V for (**1**)$Fe^{III/IV}(OH)_2$. The pK_a values 4.1 {for (**2**)$Fe^{III}(H_2O)_2$} and 7.8 {for (**2**)$Fe^{III}(H_2O)(OH)$} are smaller than 6.55 and 10.55 for (**1**)$Fe^{III}(H_2O)_2$ and (**2**)$Fe^{III}(H_2O)(OH)$, respectively,[1a] and the formal potentials for $1e^-$ oxidation of (**2**)$Fe^{III}(X)_2$ are more positive. The increase in potentials on changing the porphyrin ligand from $\mathbf{1}^{2-}$ to $\mathbf{2}^{2-}$ are 290 mV for (**porph**)$Fe^{III/IV}(H_2O)_2$, 240 mV for (**porph**)$Fe^{III/IV}(H_2O)(OH)$, and 290 mV for (**porph**)-$Fe^{III/IV}(OH)_2$. The results are reasonable if one compares the inductive effects of the eight 2,6-dichloro substituents of (**2**)H_2 and the eight 2,6-dimethyl substituents of (**1**)H_2.

The pH dependence of E_m for the reduction of (**2**)$Fe^{III}(X)_2$ is shown in Figure 3. Electrochemical and spectroelectrochemical results indicate that the reduction of (**2**)$Fe^{III}(X)_2$ to (**2**)$Fe^{II}(X)$ is not accompanied by thermodynamic axial ligand equilibration within the time scale of the electrochemical experiments used (scan rate, 20–200 mV/s) (Figure 3a). This observation is similar to the observations for the $1e^-$ reduction of (**1**)$Fe^{III}(X)_2$.[1a] Due to the change of ligation on reduction the acid dissociation constant for the water ligand of (**2**)$Fe^{II}(H_2O)$ could not be precisely measured, but the apparent formal potentials of (**2**)$Fe^{II}(H_2O)$ and (**2**)$Fe^{II}(OH)$ seem to be –0.07 and –0.27 V, respectively. The second reduction of (**2**)$Fe^{III}(X)_2$ is pH independent with E_m at –0.95 V (Figure 3b). This pH independence of half-wave potential indicates that the second $1e^-$ reduction may be assigned to the reduction of the porphyrin ring {(**2**)$Fe^{II}(X) + e^- \rightleftarrows (\mathbf{2}^{\bullet+})Fe^{II}$-(X)}.

(14) (a) Groves, J. T.; Haushalter, R. C.; Nakamura, M.; Nemo, T. E.; Evans, B. J. *J. Am. Chem. Soc.* **1981**, *103*, 2884. (b) Calderwood, T. S.; Lee, W. A.; Bruice, T. C. *J. Am. Chem. Soc.* **1985**, *107*, 8272.

Scheme III

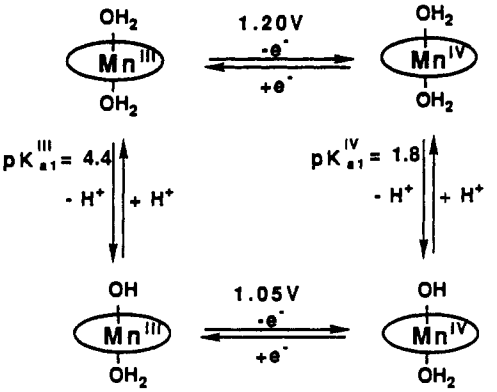

The decrease of pK_{a1} with an increase in the oxidation state of iron is as expected and has precedence in studies with (**1**)-$Fe^{III}(X)_2$.[1] The pH independence of the electrode potentials in the oxidation of (**2**)$Fe^{IV}(X)_2$ and reduction of (**2**)$Fe^{II}(X)$ is explained on the basis that the electron is removed and added, respectively, from the porphyrin ring rather than the metal. Also, the electron deficiency is delocalized on the porphyrin 24-atom framework.

Redox Chemistry of (2)$Mn^{III}(X)_2$. The dependence of half-wave potential for oxidation of (**2**)$Mn^{III}(X)_2$ upon pH is shown in Figure 4. The line generated to fit the experimental points was obtained by computer fitting of the appropriate Nernst–Clark equation (similar to that shown for (**2**)$Fe^{III}(X)_2$ in Scheme I). For comparison the dashed line represents the pH dependence of E_m for $1e^-$ oxidation of (**1**)$Mn^{III}(X)_2$ (Figure 4). The acid dissociation constants for (**2**)$Mn^{III}(H_2O)_2$ and (**2**)$Mn^{IV}(H_2O)_2$ obtained from the best fit of the appropriate Nernst–Clark equation to the experimental points are included in Scheme III.

From the dependence of E_m on pH, the pK_{a1} of (**2**)$Mn^{III}(H_2O)_2$ was measured to be 4.4 ± 0.2, but the pK_{a2} for ionization of (**2**)$Mn^{III}(HO)(H_2O)$ could not be determined electrochemically because of the HO^- envelope. For comparison the acid dissociation constants (pK_{a1} and pK_{a2}) for (**1**)$Mn^{III}(H_2O)_2$ are 5.8 and 12.2, respectively.[1a] The half-wave potentials at the two pH-independent regions in the plot of E_m vs pH for $1e^-$ oxidation of (**1**)$Mn^{III}(X)_2$ can be thought of as apparent formal potentials ($E°'$) for the oxidation–reduction equilibria between (**2**)Mn^{III}-$(X)_2$ and (**2**)$Mn^{IV}(X)_2$, as shown in Scheme III. For comparison the apparent formal potentials for $1e^-$ oxidation of (**1**)$Mn^{III}(X)_2$ are 1.04 V for (**1**)$Mn^{III/IV}(H_2O)_2$ and 0.93 V for (**1**)$Mn^{III/IV}$-$(H_2O)(OH)$. The $pK_{a1}{}^{III}$ value (4.4) of (**2**)$Mn^{III}(H_2O)_2$ is smaller than the corresponding constant (5.8) of (**1**)$Mn^{III}(H_2O)_2$, and the formal potentials for $1e^-$ oxidation of (**2**)$Mn^{III}(X)_2$ are more positive {160 mV for (**porph**)$Mn^{III/IV}(H_2O)_2$ and 120 mV for (**porph**)$Mn^{III/IV}(H_2O)(OH)$} than those of (**1**)$Mn^{III}(X)_2$. The results are consistent with the electrochemical results of water-soluble iron porphyrins {(**2**)$Fe^{III}(X)_2$ and (**1**)$Fe^{III}(X)_2$}.

Redox Chemistry of (2)$Cr^{III}(X)_2$. The pH dependence of the half-wave potentials is shown in Figure 5. The lines generated to fit the experimental points were obtained by computer fitting of the appropriate Nernst–Clark equations (similar to that shown for (**2**)$Fe^{III}(X)_2$ in Scheme I). For comparison the Nernst–Clark plots for oxidation of (**1**)$Cr^{III}(X)_2$ are given in Figure 5 as dashed lines. The dependence of the electrode potentials of (**2**)$Cr^{III}(X)_2$ upon pH can be discussed in terms of the oxidation–reduction and acid–base equilibria provided in Scheme IV. The acid dissociation constants for (**2**)$Cr^{III}(H_2O)_2$, (**2**)$Cr^{IV}(H_2O)_2$, and (**2**)$Cr^{V}(H_2O)_2$ given in Scheme IV were obtained from the best fit of the appropriate Nernst–Clark equation to the experimental points.

The electrochemically measured pK_{a1} of 8.0 ± 0.2 for acid dissociation of (**2**)$Cr^{III}(H_2O)_2$ compares favorably to the value

Scheme IV

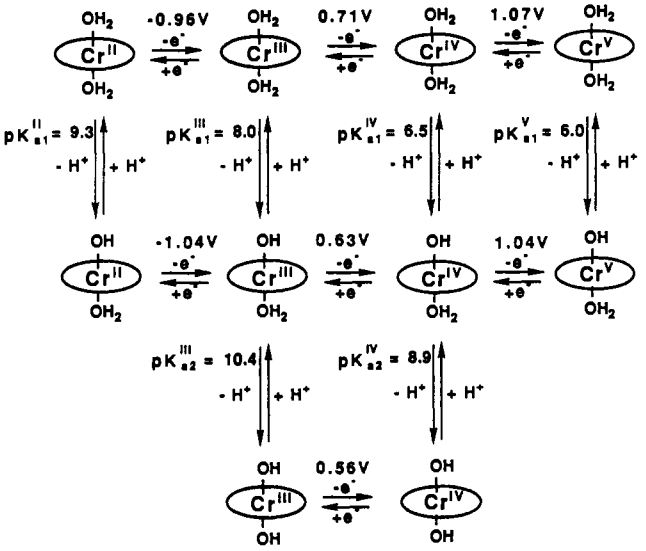

determined by spectrophotometric titration (8.1 ± 0.1) at an ionic strength of 0.2. The second constant for acid dissociation of $(2)Cr^{III}(H_2O)_2$ (pK_{a2} = 10.4 ± 0.2) was determined electrochemically but could not be observed on spectrophotometric titration. The half-wave potentials at the three pH-independent regions in the plot of E_m vs pH for 1e⁻ oxidation of $(2)Cr^{III}(X)_2$ (Figure 5) affords the apparent formal potentials ($E°'$) of Scheme IV. For comparison the apparent formal potentials for 1e⁻ oxidation of $(1)Cr^{III}(X)_2$ are 0.61 V for $(1)Cr^{III/IV}(H_2O)_2$, 0.50 V for $(1)Cr^{III/IV}(H_2O)(OH)$, and 0.39 V for $(1)Cr^{III/IV}(OH)_2$. The pK_a values (8.0 and 10.4) of $(2)Cr^{III}(H_2O)_2$ are smaller than 9.4 and 12.4 of $(1)Cr^{III}(H_2O)_2$,[1b] and the formal potentials for 1e⁻ oxidation of $(2)Cr^{III}(X)_2$ are more positive {100 mV for **(porph)**$Cr^{III/IV}(H_2O)_2$, 130 mV for **(porph)**$Cr^{III/IV}(H_2O)(OH)$, and 170 mV for **(porph)**$Cr^{III/IV}(OH)_2$} than those of $(1)Cr^{III}(X)_2$. These results are consistent with the corresponding electrochemical results obtained on comparison of the 1^{2-} and 2^{2-} ligated $Fe^{III/IV}$ hydrates. The dependence of half-wave potential upon pH (Figure 5b) is in accord with $(2)Cr^{IV}(X)_2$ undergoing metal-centered oxidation to $(2)Cr^{V}(X)_2$.

The initial oxidation product {$(2)Cr^{IV}(X)_2$} of $(2)Cr^{III}(X)_2$ does not undergo a chemical transformation to chromium(III) porphyrin π-cation radical species during the scanning time, as occurs on oxidation of $(1)Cr^{III}(X)_2$ (eqs 1–3).[1b] The greater stability

$$(1)Cr^{IV}(X)(OH) + H^+ \rightarrow (1)Cr^{IV}(X)(OH_2) \quad (1)$$

$$(1)Cr^{IV}(X)(OH_2) \rightarrow (1^{\bullet+})Cr^{III}(X)(OH_2) \quad (2)$$

$$(1)Cr^{IV}(X)(OH_2) + ClO_4^- \rightarrow (1^{\bullet+})Cr^{III}(X)(ClO_4) + H_2O \quad (3)$$

of $(1^{\bullet+})Cr^{III}(X)_2$, compared to $(2^{\bullet+})Cr^{III}(X)_2$, may be qualitatively explained by the difference in electron density on the porphyrin π-ring systems. Thus, the eight electron-withdrawing *o*-chloro groups of $(2)Cr^{IV}(X)_2$ decrease the electron density on the porphyrin ring, which destabilizes the porphyrin π-cation radical.

Table I. Differences between the Half-Wave Potential for 1e⁻ Oxidation (ΔE_m) and the First Acid Dissociation Constant (ΔpK_{a1}) When $(2)M^{III}(H_2O)_2$ and $(1)M^{III}(H_2O)_2$ {H_2O solv, μ = 0.2} Are Compared

metalloporphyrin	ΔE_m (mV)	ΔpK_{a1}
iron	290	2.4
manganese	160	1.4
chromium	100	1.4

The pK_{a1}^{II} for $(2)Cr^{II}(H_2O)_2$ was measured to be 9.3 ± 0.2, compared with the pK_{a1}^{II} of 10.6 for $(1)Cr^{II}(H_2O)_2$.[1b] The apparent formal potentials (–0.96 and –1.04 V) for the reduction of $(2)Cr^{III}(X)_2$ are also more positive than those (–1.04 and –1.13 V) for $(1)Cr^{III}(X)_2$. The decrease in the first pK_a's with increase in the oxidation state of chromium is qualitatively the same as observed for the $(2)Fe(X)_2$ system.

Influence of Electronic Effects on the pK_a and Electrode Potential in the Tetraphenylporphyrin Moiety. In nonaqueous media half-wave potentials of metalloporphyrins have been shown to depend on overall porphyrin basicity.[15] The effect of substituents on the electrode reactions of substituted iron tetraphenylporphyrins has been carried out in aqueous and nonaqueous solutions.[16] Electron-withdrawing substituents produce a more easily reduced form, as evidenced by an anodic shift of the reversible half-wave potentials. Also, the ring oxidations and ring reductions were observed to be considerably more sensitive to substituents than was the metal-centered reaction. From the present study in aqueous solutions, the shift in the half-wave potential (ΔE_m) for 1e⁻ oxidation of $(2)M^{III}(H_2O)_2$ (M = Fe, Mn or Cr) compared to that of $(1)M^{III}(H_2O)_2$ as well as the change in pK_{a1} (ΔpK_{a1}) of H_2O axial ligand are summarized in Table I. The more positive values of the half-wave potentials of $(2)M^{III}(X)_2$, compared to those of $(1)M^{III}(X)_2$, relate to the greater electron-withdrawing by *o*-chloro as compared to *o*-methyl substituents. From Table I it follows that the sensitivity of the positive nature of M(III) to electron withdrawal from the porphyrin ligand follows the sequence Fe(III) > Mn(III) > Cr(III).

Impact on Previous Investigations. In previous investigations[9a] we assumed that the only spectrophotometrically determined pK_a values of 6.6 with $(1)Fe^{III}(X)_2$ and 7.6 with $(2)Fe^{III}(X)_2$ pertained to the acid dissociation of $(1)Fe^{III}(H_2O)_2$ and $(2)Fe^{III}(H_2O)_2$, respectively. If this were true, the H_2O ligand of the more electron deficient $(2)Fe^{III}(H_2O)_2$ would be the least acidic. To explain this apparent anomaly we invoked the influence of a field effect on the ligated water by the closely adjacent –Cl functions. The present study established that the first pK_a of $(2)Fe^{III}(H_2O)_2$ at 4.1 is spectrophotometrically invisible such that the H_2O ligand of the more electron deficient $(2)Fe^{III}(H_2O)_2$ is more acidic than the H_2O ligand of $(1)Fe^{III}(H_2O)_2$. The discussion concerning the invoked field effect in ref 9a is withdrawn.

Acknowledgment. This work was supported by a grant from the National Institutes of Health.

(15) (a) Walker, F. A.; Beroiz, D.; Kadish, K. M. *J. Am. Chem. Soc.* **1976**, *98*, 3484. (b) Kadish, K. M.; Morrison, M. M. *Inorg. Chem.* **1976**, *15*, 980. (c) Kadish, K. M. *Prog. Inorg. Chem.* **1986**, *34*, 435.

(16) (a) Kadish, K. M.; Morrison, M. M.; Constant, L. A.; Dickens, L.; Davis, D. G. *J. Am. Chem. Soc.* **1976**, *98*, 8387. (b) Giraudeau, A. G.; Callot, H. J.; Jordan, J.; Ezhar, I.; Gross, M. *J. Am. Chem. Soc.* **1979**, *101*, 3857. (c) Giraudeau, A. G.; Callot, H. J.; Gross, M. *Inorg. Chem.* **1979**, *18*, 201. (d) Ni, C.-L.; Anson, F. *Inorg. Chem.* **1985**, *24*, 4754. (e) Su, Y. O.; Kuwana, T.; Chen, S.-M. *J. Electroanal. Chem. Interfacial Electrochem.* **1990**, *288*, 177.